


Qualitative and quantitative nature of mutual interactions dictate chemical noise in a democratic reaction network

Soutrick Das  and Debashis Barik ^{*}

School of Chemistry, University of Hyderabad, Gachibowli, 500046 Hyderabad, India

 (Received 30 November 2019; revised manuscript received 24 February 2020; accepted 16 March 2020; published 17 April 2020)

The functions of a living cell rely on a complex network of biochemical reactions that allow it to respond against various internal and external cues. The outcomes of these chemical reactions are often stochastic due to intrinsic and extrinsic noise leading to population heterogeneity. The majority of calculations of stochasticity in reaction networks have focused on small regulatory networks addressing the role of timescales, feedback regulations, and network topology in propagation of noise. Here we computationally investigated chemical noise in a network with democratic architecture where each node is regulated by all other nodes in the network. We studied the effects of the qualitative and quantitative nature of mutual interactions on the propagation of both intrinsic and extrinsic noise in the network. We show that an increased number of inhibitory signals lead to ultrasensitive switching of average and that leads to sharp transition of intrinsic noise. The intrinsic noise exhibits a biphasic power-law scaling with the average, and the scaling coefficients strongly correlate with the strength of inhibitory signal. The noise strength critically depends on the strength of the interactions, where negative interactions attenuate both intrinsic and extrinsic noise.

DOI: [10.1103/PhysRevE.101.042407](https://doi.org/10.1103/PhysRevE.101.042407)

I. INTRODUCTION

Robustness and reliability are key to living organisms with respect to their responses to various internal and external cues and to their long-term survival. Stochasticity of chemical reactions originating from intrinsic and extrinsic sources hampers these two important aspects of living systems. Therefore a considerable number of efforts have been made to understand the ways living systems regulate the stochasticity which ultimately leads to population heterogeneity, an unavoidable natural phenomena of genetically identical cells under homogeneous environmental conditions [1,2]. The fluctuations of a finite number of macromolecular species in the cellular compartment result in stochastic trajectories of chemical reactions inside the cell. This finite number effect of molecular abundance is intrinsic to a chemical reaction. Owing to the intrinsic noise, the expression of a gene was found to be noisy and was termed gene expression noise [3–6]. However, variation in other factors, such as cell size, volume, cell cycle phase, and concentration of key regulators, acts as another source of noise and was collectively known as extrinsic noise that influences all chemical reactions inside a cell identically [4,6–10]. In the majority of the cases, the chemical noise, a term commonly used to reference both types of noise, leads to an inconsequential population heterogeneity of various cellular properties, for example, events in a cell cycle [11], variability in key signaling events [12,13], and desynchrony in oscillatory response [14]. However, in some cases the heterogeneity was found to be beneficial for the

living organisms [15,16]. For example, under stress the gene expression noise allows single-cell organisms to adapt to the altered conditions efficiently, and ultimately it helps the organisms to thrive in an unfavorable environment via phenotypic diversity [17–19].

Statistical mechanical models of a single gene or a few genes in a cascade have been successful in providing great insight into the mechanisms of gene expression noise [20–27]. These models have highlighted the roles of disparity in the average lifetime of proteins and mRNAs and translational and transcriptional bursting in gene expression noise. Further investigations were carried out to decipher the role of feedback regulations in attenuating or amplifying biochemical noise. Early studies revealed that negative feedback has the potential to reduce the noise, whereas positive feedback amplifies noise [20,28–30], although later calculations exhibited that positive feedback also has the potential to reduce noise [31,32]. Horizons of these calculations were further extended with the investigations of the role of network topology in noise propagation [33–41]. In this context, we have recently shown that parallel arrangements of interconnected positive feedback loops efficiently reduce chemical noise as compared to serial arrangements of positive feedback loops [42].

Although a plethora of literature is available on the propagation of chemical noise in biochemical reaction networks, investigation of stochasticity in a generalized network is, however, lacking. Particularly it is worth noting that the system-level response of a living cell relies on coordinated expression of multiple genes interconnected with each other. An interesting aspect of these gene regulatory networks is the global architecture of the networks [43–45]. Recent literature suggests that often these networks exhibit a resemblance

^{*}dbariksc@uohyd.ac.in

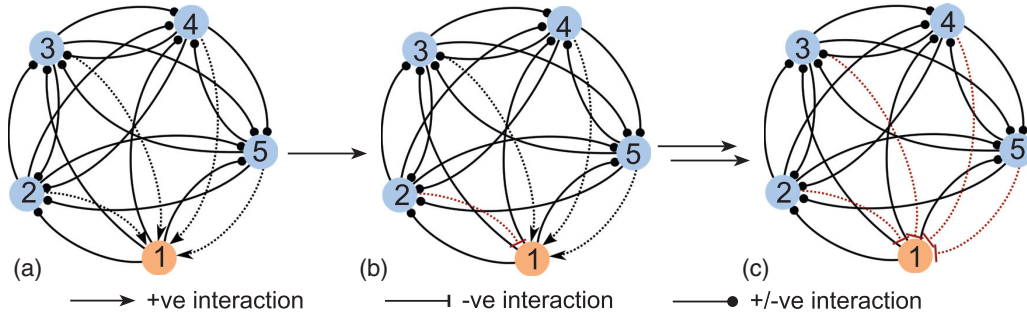


FIG. 1. (a) Schematic diagram democratic network with five nodes ($d_N = 5$). The numbered circles and the curved lines represent the nodes and connectivity among the nodes, respectively. The different types of arrowheads represent types of interactions. Pointed arrowhead: positive interaction; blunt head: negative interaction; and circular arrowhead: either positive or negative interaction. In this particular network, all other nodes act positively on node 1, and interaction on all other nodes could be positive or negative depending on the value of $m_{i \neq 1}^+$ and $m_{i \neq 1}^-$. (b) and (c) Systematic modification of the number of negative interaction on node 1.

to a democratic network where each gene is regulated by other genes (or gene product) in the network [46]. Here we investigated the variability due to both intrinsic and extrinsic noise in democratic chemical reaction networks. Our objective was to study the correlation between the variability and the qualitative (inhibitory or activatory) and quantitative (strength) nature of mutual interactions in the network. Using numerical simulations, we estimated noise in a democratic chemical reaction network in a systematic manner by varying the number of inhibitory (negative) and activatory (positive) interactions. In order to estimate the effect of intrinsic noise we used Gillespie's stochastic simulation algorithm (SSA) [47], whereas to estimate the effect of extrinsic noise we simulated the corresponding deterministic dynamical equations of an ensemble of networks. We found that with the variation of the number of negative interactions on a node, the average abundance behaved like an ultrasensitive switch. Due to the sharp switching of the average, the intrinsic chemical noise exhibited a biphasic power-law scaling with the average. The scaling exponents were strongly dependent on the average strengths of the positive and negative interactions in the network. Further the negative regulations acted as a noise attenuator in the network. Calculations of networks with only extrinsic noise revealed similar roles of negative regulators in the democratic chemical reaction networks.

II. MODEL AND RESULTS

Our network model consists of nodes interconnected by edges. These nodes could be proteins or genes or transcripts or metabolites. The nodes are the representatives of any macromolecular species present inside a living cell, whereas the edges represent the nature of the interaction between the two connected nodes. The interaction between the two nodes could be either negative (inhibitory) or positive (activatory). Every node in the network consists of a certain number of incoming and outgoing edges represented by the arrowhead types [Fig. 1(a)]. Incoming arrows indicate the influence of other nodes on the recipient node, whereas the outgoing arrows indicate the influence of the source node on the recipient nodes in the network. In a democratic network, we assume that the number of incoming and outgoing interactions are same on every node in the network. This means that every node

receives inhibitory or activatory signals from all the rest of the nodes in the network. Therefore, in a democratic network with d_N number of nodes, the total number of interactions (m_{tot}) on any node would be $d_N - 1$. In addition to these interactions from other nodes, every node has its own unregulated synthesis and degradation. Assuming the mass action rate laws of chemical reactions, the mean field dynamics of the nodes can be represented by a set of coupled ordinary linear differential equations:

$$\frac{d\bar{n}_i}{dt} = k_i - \gamma_i \bar{n}_i + \sum_{i \neq j}^{d_N} a_{i,j} \bar{n}_i \bar{n}_j. \quad (1)$$

In the above equation \bar{n}_i is the average abundance, in numbers of molecules, of the node i . On the right-hand side of the equation, the first and the second terms are the unregulated synthesis and degradation of the i th node, respectively. k_i and γ_i are the associated rate constants with the synthesis and degradation reactions, respectively. The last term represents the mutual bimolecular interaction between node i and node j . While the numerical value of $a_{i,j}$ represents the strength of the interaction, its sign indicates the qualitative nature of interaction. $a_{i,j} < 0$ and $a_{i,j} > 0$ represent inhibitory and activatory interactions, respectively. By varying the number of negative (m_i^-) and positive (m_i^+) interactions on every node, one can generate a large number of different network models. Note that the total number of interaction on every node is fixed to $m_{\text{tot}} (= m_i^- + m_i^+)$. It turns out that a democratic network of d_N nodes consists of $d_N(d_N - 1)$ number of mutual interactions.

For every node in the network, we chose a fixed value of the basal synthesis rate constant ($k_i = 1.0$) and the degradation rate constant ($\gamma_i = 0.01$). However, the strength of the mutual interaction ($a_{i,j}$) was chosen to be different for every pair of interacting nodes (i, j). In order to create variation in the strength of interactions, we picked $a_{i,j}$ from log-normal distributions with average values of \bar{a}_- (for negative interactions) and \bar{a}_+ (for positive interactions) with a coefficient of variation of 0.3 in both cases. It is important to note that one can choose the values of the interaction parameters from any distribution which can be realistically associated with the reaction networks. However, the conclusions must not be skewed by the choice of the distribution for $a_{i,j}$. In this

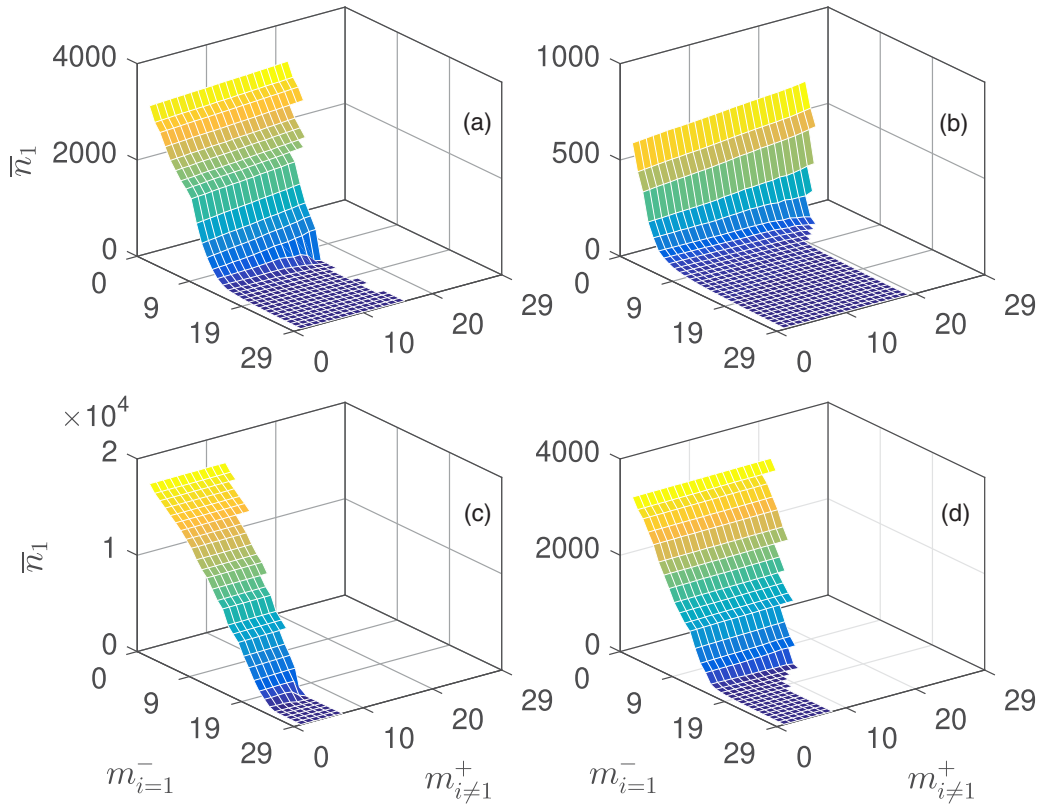


FIG. 2. Surface plot of the average abundance of node 1 (\bar{n}_1) as a function of the number of negative interactions on node 1 ($m_{i=1}^-$) and the number of positive interactions on the rest of the nodes ($m_{i \neq 1}^+$), for different combinations of average strengths of negative and positive interactions (\bar{a}_- , \bar{a}_+). (a) (0.001, 0.001), (b) (0.005, 0.001), (c) (0.001, 0.005), and (d) (0.005, 0.005).

context we have verified that the conclusions of our studies remain the same with the use of Gaussian distribution for $a_{i,j}$ (see Fig. 18). The sample size for the distribution was $d_N(d_N - 1)$ as there were that many numbers of binary interactions available in the network. The choice of a log-normal distribution for interaction strengths resulted in an asymmetric network in terms of the strength of the interactions. We systematically varied \bar{a}_- and \bar{a}_+ to determine the effects of strengths of interactions on the statistical properties of the network.

Our goal was to investigate the effect of negative and positive interactions on the steady-state variability of the chemical species in democratic networks. For this purpose, we studied networks with a different number of negative and positive interactions. Due to the democratic nature of the network all nodes are equivalent, therefore one can choose any node in the network to study statistical properties such as mean, noise (coefficient of variation), and noise strength (Fano factor) of the network. Here we chose node 1 as a candidate for our investigations. In order to determine the effect of negative interaction on noise, we systematically increased the number of negative interaction on node 1 ($m_{i=1}^-$), and in each case we quantified steady-state statistical properties of node 1 and as well as all other nodes in the network. This allowed us to determine the dependence of statistical properties of node 1 on the nature of incoming interactions on it. In Figs. 1(b) and 1(c) we represent the scheme of systematic variation of $m_{i=1}^-$ on node 1. In performing these calculations we kept the number of negative ($m_{i \neq 1}^-$) and positive ($m_{i \neq 1}^+$) interactions of

all other nodes ($i \neq 1$) fixed. In order to determine the effect of the nature of interactions of the rest of the nodes ($i \neq 1$) on the statistical properties of node 1, we repeated the mentioned set of calculations with systematic variation of $m_{i \neq 1}^+$.

A. Intrinsic noise

Intrinsic noise originates from the fluctuations of the finite number of molecular species present inside a living cell, and it leads to stochastic trajectories of chemical reactions [1]. In order to investigate the intrinsic noise, we simulated the chemical reactions corresponding to the model equations (1). Owing to the linearity of the dynamical equations, the corresponding chemical reactions follow mass action rate laws. There are d_N number of synthesis, d_N number of degradation, and $d_N(d_N - 1)$ number of interaction reactions in the network. Therefore, the total number of chemical reactions in the network becomes $d_N(d_N + 1)$. We used Gillespie's SSA [47] to simulate the chemical reactions associated with the network model. We ran simulations for a sufficiently long time to ensure that the trajectories reached their steady states. Further, in order to obtain accurate statistics, we ran simulations for 5000 trajectories for ensemble average. We kept the values of $a_{i,j}$ fixed in the every run of the simulations. Generally with increased network size (d_N) and with higher values of rate constants, the simulation run time increases steeply in SSA. Therefore to cut down the simulation time, we imposed a cutoff abundance of 100 000 molecules/node. According to the cutoff rule, the simulation stops when the abundance of any

node reached the cutoff value. Use of 100 000 molecules/node as cutoff was not completely unreasonable as the noise associated with this would be very small based on the $1/\sqrt{\bar{n}_i}$ rule of molecular fluctuations. In the following we report results for networks with $d_N = 30$. However, we have also verified that our conclusions are consistent for network with $d_N = 20$ and $d_N = 10$.

In Fig. 2(a) we present the variation of the average abundance of node 1 (\bar{n}_1) with the increasing number of negative interactions on it ($m_{i=1}^-$) and increasing number of positive interactions on all other nodes ($m_{i\neq 1}^+$) in the network keeping the average strengths of negative and positive interactions the same. Expectedly, for a given value of $m_{i\neq 1}^+$ the average abundance of node 1 decreased with $m_{i=1}^-$. We obtained similar qualitative behavior of \bar{n}_1 when we repeated calculations with a systemic increase of $m_{i\neq 1}^+$ in the network [surface plot in Fig. 2(a)]. It is interesting to note that \bar{n}_1 changed barely with the increase of $m_{i\neq 1}^+$. However, for large $m_{i\neq 1}^+$ (>15), the system became divergent, and due to the cutoff rule the surface plot do not have data points for node 1 in those cases. Therefore our simulations indicate that the qualitative or quantitative nature of \bar{n}_1 is regulated by the signs of $a_{1,j}$ not by $a_{i\neq 1,j}$ (at least in the chosen parameter set). We point out here that, for the sake of ease in implementation, we increased the number of negative interactions on node 1 in a specific order. In particular, we always increased the number of negative interaction starting from node 2. Similarly, we also followed a specific order to increase the number of positive interactions on all other nodes. However we have confirmed that the results are independent of the specific nodes chosen to implement a negative or positive effect on node 1.

In order to determine how the average depends on the strength of the negative or positive interactions, we performed calculations with different average strengths of interactions. In Figs. 2(b)–2(d) we present the effect of five times increased strengths of negative [Fig. 2(b)], positive [Fig. 2(c)], and both [Fig. 2(d)] of the interactions. With an increased value of \bar{a}_- alone, the average abundance of node 1 decreased across the various numbers of both types of interactions. In addition, a smaller number of negative interactions ($m_{i=1}^-$) were sufficient to “shut down” node 1. On the other hand, with an increased value of \bar{a}_+ alone, \bar{n}_1 increased significantly and more number of negative interactions were needed to stop the production of node 1. In addition the divergence of abundance happened in a much smaller value of $m_{i\neq 1}^+$. Finally when both the strengths were increased by the same factor, only a marginal change occurred in \bar{n}_1 .

It appears from Fig. 2 that the average of node 1 (\bar{n}_1) was reduced abruptly from high to low beyond a critical number of $m_{i=1}^-$. Thus the qualitative variation of \bar{n}_1 with $m_{i=1}^-$ behaved like an ultrasensitive switch of protein activity in biochemical networks [48]. It is worth noting that ultrasensitivity in biochemical systems is often due to the intrinsic nonlinearity of the underlying chemical reactions. However, here we report a weak ultrasensitivity due to the democratic architecture of the network that does not possess nonlinear rates of chemical reactions. The importance of ultrasensitivity in biochemical reaction networks is enormous due to its relevance in generating nonlinear responses such as bistability and oscillations [49]. Therefore we next investigated further the conditions

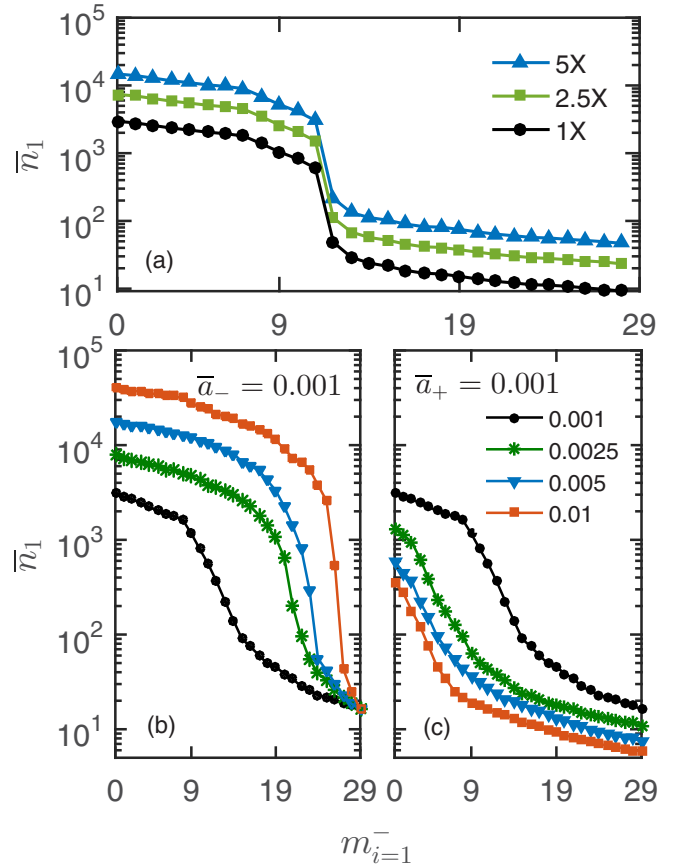


FIG. 3. (a) Dependence of the ultrasensitivity of node 1 on the scaling factors that systematically modifies that average abundance of all the nodes in the network. The values of \bar{a}_+ and \bar{a}_- were 0.001 and 0.001, respectively. (b) Dependence of the ultrasensitivity on the average strength of positive interactions keeping the \bar{a}_- fixed. (c) Dependence of the ultrasensitivity on the \bar{a}_- keeping the \bar{a}_+ fixed.

of ultrasensitive switching of node 1. In order to address the question that the switchlike behavior of node 1 was not due to the very few molecules in high $m_{i=1}^-$, we systematically scaled up the abundance of the nodes by 2.5 \times and 5.0 \times . In order to scale up the abundance we multiplied and divided the zero- and second-order rate constants, respectively, by the appropriate scaling factor. The ultrasensitive switching of node 1 remained intact even with higher population abundance indicating that the ultrasensitivity is the intrinsic property of the democratic network [Fig. 3(a)]. Simulations from different average strengths of positive and negative interactions indicate that the stiffness of the switch depends on the average strength of the positive interactions. On the other hand, the strength of the negative interaction seems to control the transition threshold of $m_{i=1}^-$ [Figs. 3(b) and 3(c)].

Having established the average behavior of the democratic network, we next looked at the effect of negative interactions on the noise in node 1. Here we quantified the coefficient of variation ($CV = \sigma_i/\sqrt{\bar{n}_i}$; σ_i = standard deviation) as a measure of noise at steady state. At equal strengths of negative and positive interactions, the noise exhibited a switchlike behavior as a function of $m_{i=1}^-$ [Fig. 4(a)]. Specifically, CV remained very low for a smaller number of $m_{i=1}^-$ (high \bar{n}_1),

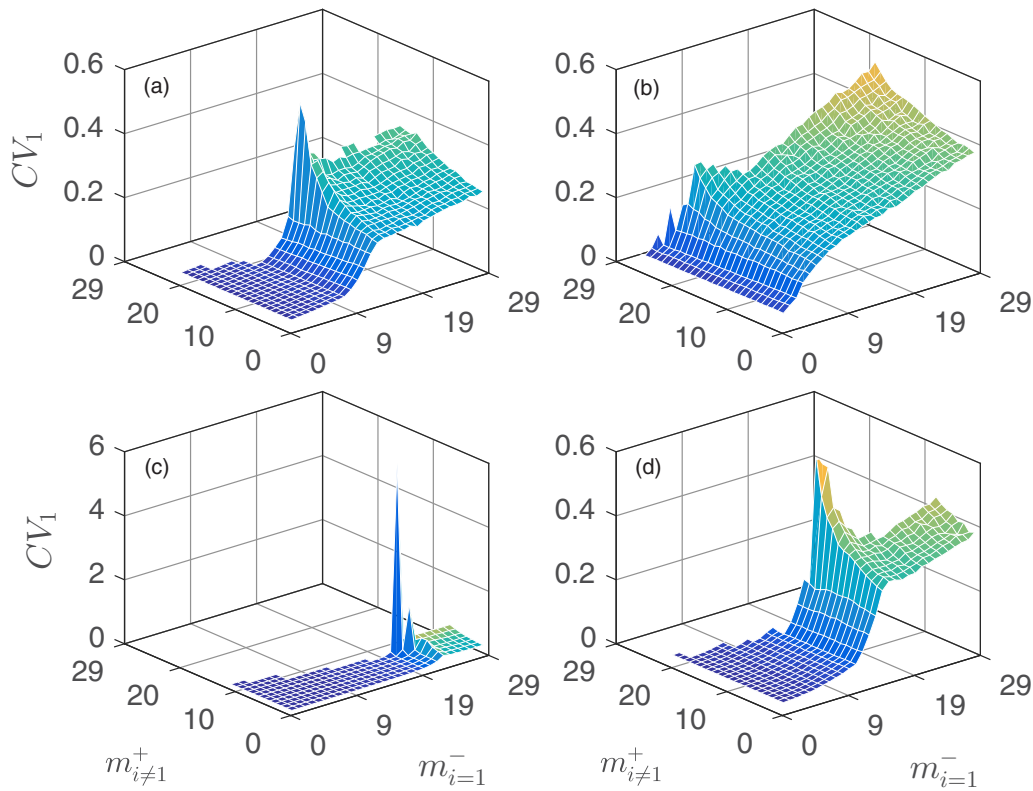


FIG. 4. Surface plot for the coefficient of variation of node 1 (CV_1) as function of $m_{i=1}^-$ and $m_{i \neq 1}^+$. The average strength of negative and positive interaction was (a) (0.001, 0.001), (b) (0.005, 0.001), (c) (0.001, 0.005), and (d) (0.005, 0.005).

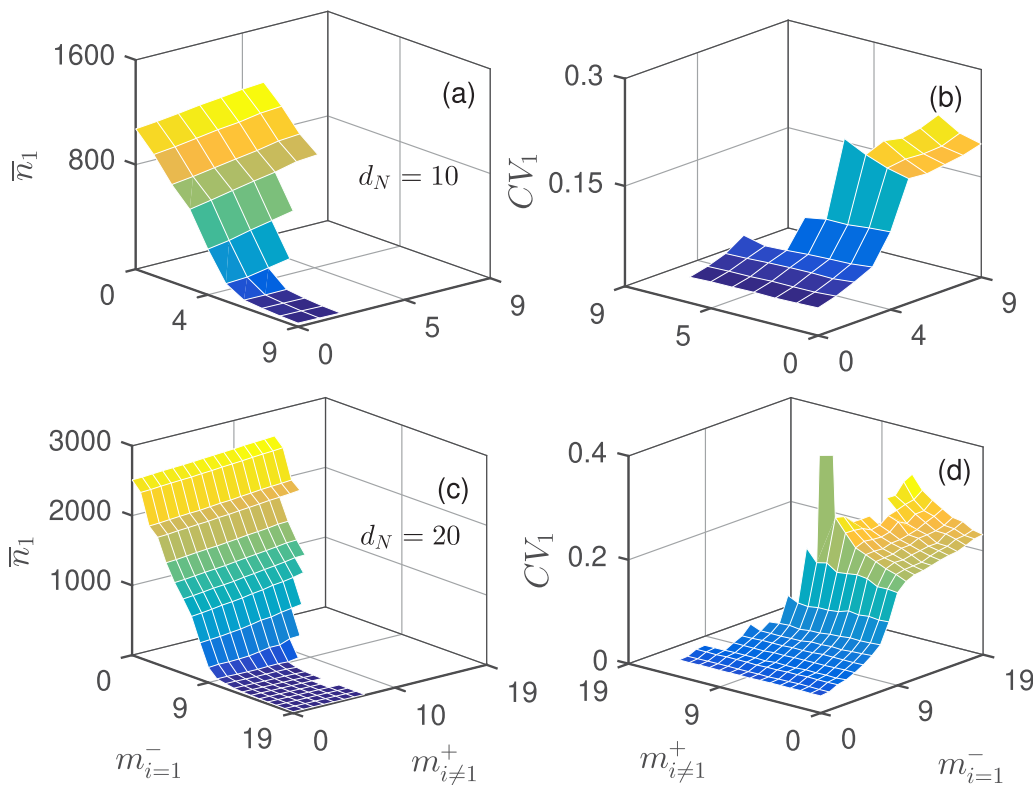


FIG. 5. Surface plot of the average abundance and CV of node 1 for the networks with 10 (top row) and 20 (bottom row) nodes as a function of $m_{i=1}^-$ and $m_{i \neq 1}^+$. The values of \bar{a}_- and \bar{a}_+ were 0.001 and 0.001, respectively

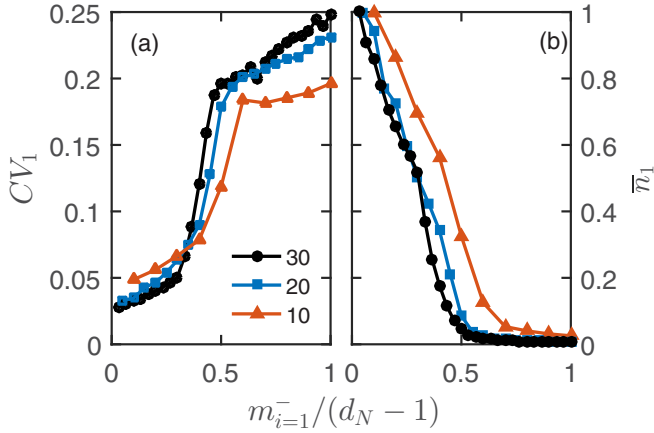


FIG. 6. Variation of CV (a) and normalized average (b) of node 1 as a function normalized $m_{i=1}^-$ ($m_{i=1}^- / (d_N - 1)$) for the indicated sizes of networks with $m_{i \neq 1}^+ = 0$. The average was normalized by dividing \bar{n}_1 by the maximum average value in each case. The values of \bar{a}_- and \bar{a}_+ were the same as in Fig. 5.

and it nearly saturated with a high value for a larger number of $m_{i=1}^-$ (low \bar{n}_1). Although this feature of noise was repeated for an increasing number of positive interactions on the other nodes ($m_{i \neq 1}^+$), however, in the high-noise regime (large $m_{i=1}^-$), the noise seemed to increase steadily with the increase of $m_{i \neq 1}^+$. Therefore, altogether direct negative interactions lead to nonmonotonous increase of noise and indirect positive interactions results in marginal increase of noise. To determine how these qualitative natures of noise depend on the strength of interactions, we repeated these calculations with different average strengths of both interactions (\bar{a}_- and \bar{a}_+). With an increased value of \bar{a}_- alone, expectedly the switching from low to high noise happened at a much lower value $m_{i=1}^-$ [Fig. 4(b)]. However, in this case the variability increased noticeably as compared to smaller \bar{a}_- [Fig. 4(a)]. This was due to the fact that higher \bar{a}_- resulted in a lower average amplifying the finite number effect. Further the effect of $m_{i \neq 1}^+$ on CV in larger values of $m_{i=1}^-$ was very prominent. With an

increased value of \bar{a}_+ only, the transition from low to high noise happened at a much larger value of $m_{i=1}^-$ [Fig. 4(c)]. Although the qualitative nature remained the same in the case where both interaction strengths were increased by the same factor [Fig. 4(d)], across various values of $m_{i=1}^-$ and $m_{i \neq 1}^+$ the noise increased noticeably as compared to the case with lower values of the strengths [Fig. 4(a)]. This was probably due to the faster propagation of noise in the network.

We ran simulations of different sizes of democratic networks to determine the universality of the qualitative nature of noise with $m_{i=1}^-$. In Fig. 5 we report the simulation results from networks with 10 and 20 nodes. In Fig. 6(a) we compare CV₁ versus $m_{i=1}^-$ of three different networks sizes ($d_N = 10, 20, 30$) where in each case the number of positive interactions on all other nodes was fixed to 0 ($m_{i \neq 1}^+ = 0$). The comparison shows that the sharp change of noise from a low to high value is indeed universal across the different network sizes. We also notice a systematic shift of the curves towards lower $m_{i=1}^-$ with increasing network size. In Fig. 6(b) we compared their respective normalized averages to note the rapid drop of the corresponding averages with $m_{i=1}^-$.

The scaling behavior of noise with the average has been an important measure in the stochastic calculations of coupled chemical reaction systems. To address this aspect, in Fig. 7(a) we plot CV₁ with \bar{n}_1 for different values of $m_{i \neq 1}^+$. Here the dependence of noise on the average is quite different from $CV \propto 1/\sqrt{\bar{n}}$ scaling, and in fact the dependence can be best fit by two independent power-law scalings (piecewise power-law, $CV \propto \bar{n}^\alpha$) with two different scaling exponents α_1 and α_2 . We fitted the linear region (in the log-log plot) of the individual lines and report the average and standard deviation of the scaling exponents. In the low to intermediate abundance regime the scaling exponent had the value of $\alpha_1 = -0.2 \pm 0.02$, whereas in the intermediate to high abundance regime it was $\alpha_2 = -0.9 \pm 0.03$. The accuracy of the fits was measured by calculating R^2 values of the individual fits. The average values of R^2 were 0.908 ± 0.05 and 0.996 ± 0.002 for α_1 and α_2 , respectively. Next we determined the scaling of node 15, a candidate node whose average was not modified directly by the systematic modification of the number of

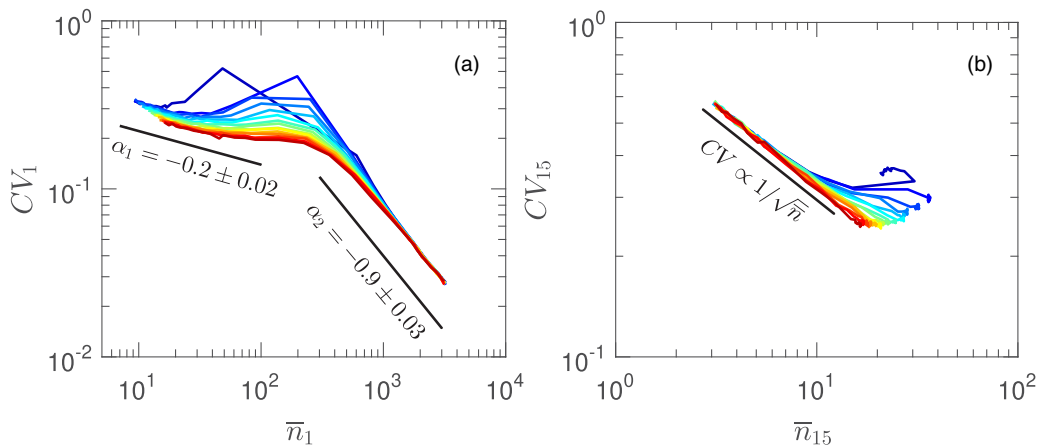


FIG. 7. Dependence of CV of node 1 (a) and node 15 (b) as a function of their respective averages. Different lines represent different values of $m_{i \neq 1}^+$: from red ($m_{i \neq 1}^+ = 0$) to blue ($m_{i \neq 1}^+ = 16$) the value of $m_{i \neq 1}^+$ increases by 1. The scaling exponents from power-law fitting ($CV_i \propto \bar{n}_i^\alpha$) of the data segment are indicated inside the plots. The values of \bar{a}_- and \bar{a}_+ were the same as in Fig. 5.

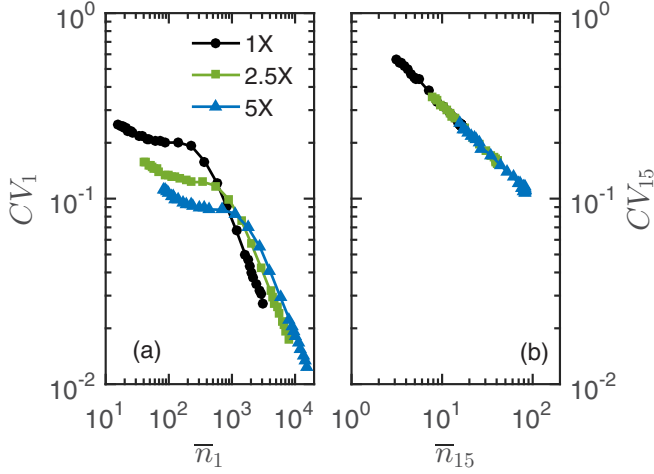


FIG. 8. Variation of biphasic behavior of noise in node 1 (left) and monophasic behavior of noise in node 15 (right) with the indicated values of scaling factors. The other parameters were $\bar{a}_+ = 0.001$, $\bar{a}_- = 0.001$, and $m_{i \neq 1}^+ = 0$.

negative regulations on node 1. We found that [Fig. 7(b)] this node exhibited the well-known scaling of $CV \propto 1/\sqrt{\bar{n}}$ across the different values of $m_{i \neq 1}^+$. Therefore it is fair to conclude that a node whose average was modified directly by negative regulations obeys the biphasic scaling of noise, whereas a node whose average was modified indirectly by negative regulations follows the usual scaling of noise.

From Fig. 7 it is clear that the range of the average abundance for node 1 was significantly larger than the range of abundance of all other nodes in the network. This poses an obvious question whether the disparity of the scaling behavior of the nodes was due to their different regime of abundance. The ranges of node 1 and other nodes were different due to the fact that the variation of $m_{i=1}^-$ caused a direct effect on node 1, whereas it resulted in an indirect effect on all other nodes in the network. In order to increase the range of abundance, we ran simulations with different scaling factors that scaled up the abundance of all nodes systematically. In Fig. 8 we plotted the CV against \bar{n} for node 1 and node 15 with different

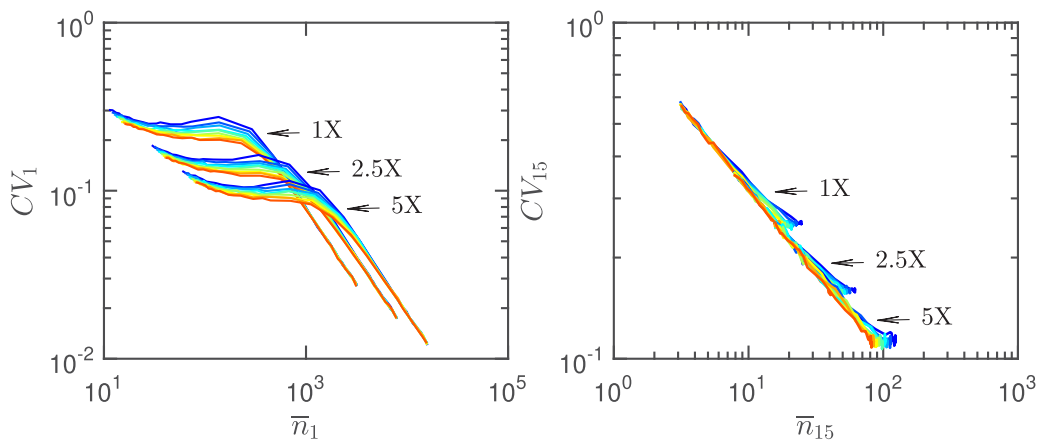


FIG. 9. Plots similar to those in Fig. 8 with different values of $m_{i \neq 1}^+$. Different lines represent different values of $m_{i \neq 1}^+$: from red ($m_{i \neq 1}^+ = 0$) to blue ($m_{i \neq 1}^+ = 8$) the value of $m_{i \neq 1}^+$ increases by 1.

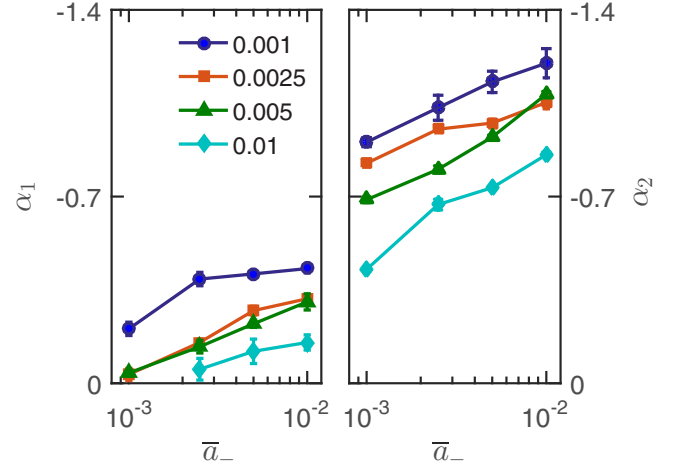


FIG. 10. Variation of scaling exponents α_1 and α_2 with the \bar{a}_- for indicated values of \bar{a}_+ .

scaling factors for the networks having $m_{i \neq 1}^+ = 0$. The shifting of the entire scaling curves to the higher abundance regime indicates the universal nature of the scaling laws of node 1 and the rest of the nodes in the democratic network. Further the universality of scaling laws was independent of $m_{i \neq 1}^+$ as similar shifts of scaling behavior were noticed for other values of $m_{i \neq 1}^+$ (Fig. 9).

In order to determine the dependence of the scaling exponents on the average strengths of negative and positive interactions, we estimated these exponents by running simulations for a range of values of \bar{a}_- and \bar{a}_+ . With the increased strength of negative interaction, we found a systematic increase of both exponents irrespective of the values of \bar{a}_+ (Fig. 10). It indicates that the effect of negative interaction on the noise is stronger for its higher strength. On the other hand, with the increased strength of positive interaction, the values of both exponents decreased irrespective of the value of the strength of negative interaction. Therefore, in general in a democratic network, negative interaction strongly regulates the noise as compared to the positive interactions.

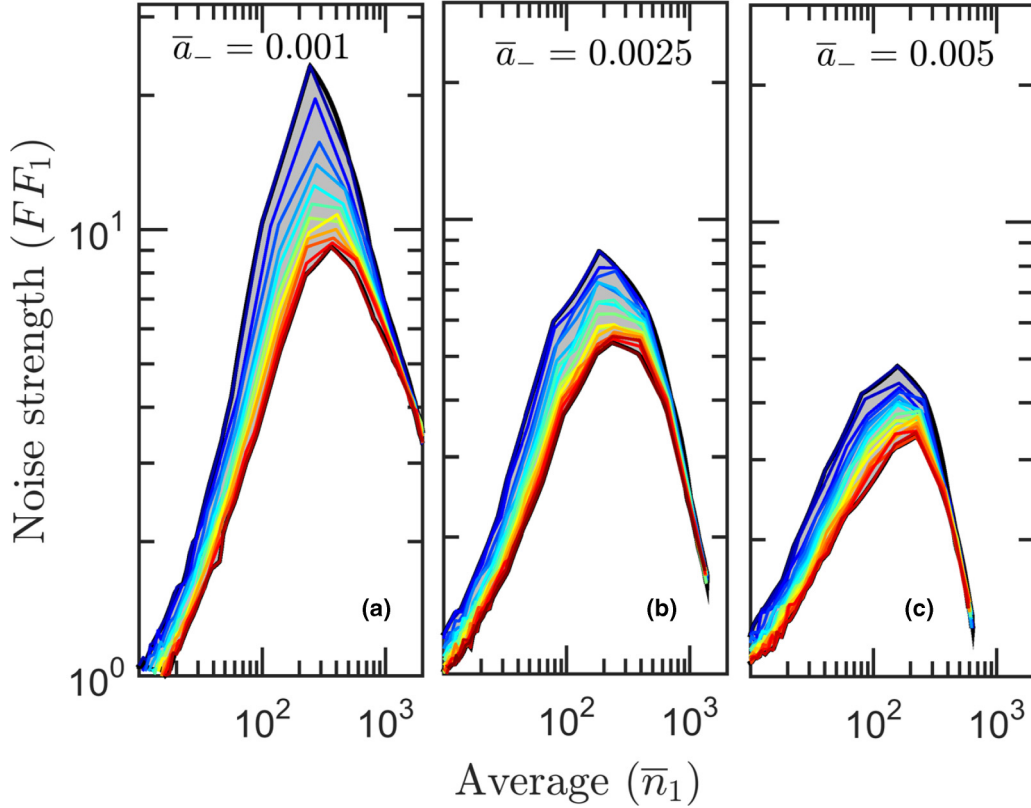


FIG. 11. Variation of noise strength (Fano factor, $FF_1 = \sigma_1^2/\bar{n}_1$) for node 1 as function of \bar{n}_1 . Different lines represent different values of $m_{i \neq 1}^+$: from red ($m_{i \neq 1}^+ = 0$) to blue ($m_{i \neq 1}^+ = 18$) the value of $m_{i \neq 1}^+$ increases by 1. In all three panels the value of \bar{a}_+ was kept fixed to 0.001.

In the context of small gene regulatory network, the role of negative regulation in attenuating noise has been explored before with a conclusion that it dampens the intrinsic noise, whereas positive regulations were found to amplify the noise. However, later investigations showed that positive regulations can also reduce noise, particularly in the context of feedback regulated systems [32]. To address this issue in the context of democratic architecture, we explored the effect of negative regulations on the noise strength. In Fig. 11(a) we plotted noise strength (also known as the Fano factor, $FF_1 = \sigma_1^2/\bar{n}_1$) of node 1, as a function of \bar{n}_1 for a different number of $m_{i \neq 1}^+$. Noise strength passed through maxima with average irrespective of the number of $m_{i \neq 1}^+$, indicating that the intermediate number of negative interactions (i.e., intermediate average) on node 1 resulted in maximum noise strength. Further the peak noise strength increased with an increased value of $m_{i \neq 1}^+$. Although the network exhibited similar qualitative behavior of FF_1 for different values of \bar{a}_- , the overall noise strength decreased with increased \bar{a}_- [Figs. 11(b) and 11(c)]. For a complete understanding of the effect of \bar{a}_- as well as $m_{i \neq 1}^-$ on the noise strength, in Fig. 12(a) we plotted the maximum value of noise strength ($^{\max}FF_1$) as a function of \bar{a}_- in the network with $m_{i \neq 1}^+ = 0$ (or $m_{i \neq 1}^- = 29$). These plots indicate that the maximum noise strength decreases with increasing strength of negative interaction irrespective of the strength of the positive interaction. The reduction of noise strength with \bar{a}_- suggests the noise attenuation capacity of negative regulations. However, with the increasing strength of positive interaction, the maximum noise strength increases consistently, indicating

that the positive interaction leads to amplification of noise strength. The plot [Fig. 12(b)] of the number of negative interactions on node 1 corresponding to the maximum noise

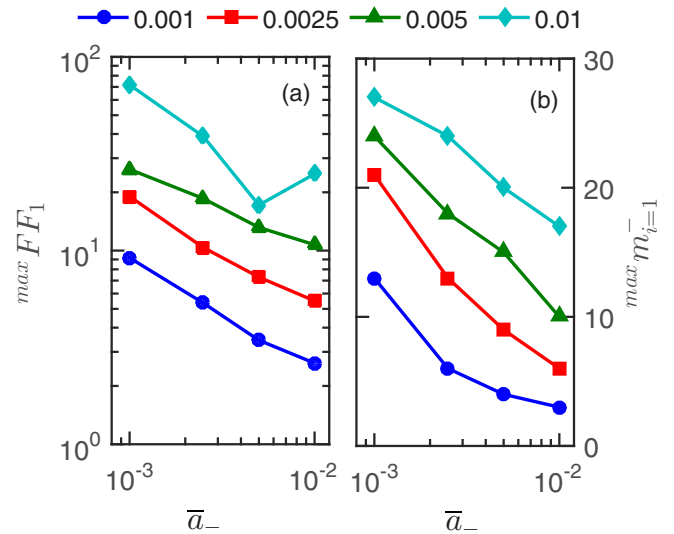


FIG. 12. (a) Dependence of maximum noise strength ($^{\max}FF_1$) (obtained from Fig. 11) with \bar{a}_- for $m_{i \neq 1}^+ = 0$. (b) Variation of $^{\max}m_{i \neq 1}^-$, the number of negative interactions on node 1 corresponding to the maximum noise strength, with \bar{a}_- . Different lines represent different values of \bar{a}_+ .

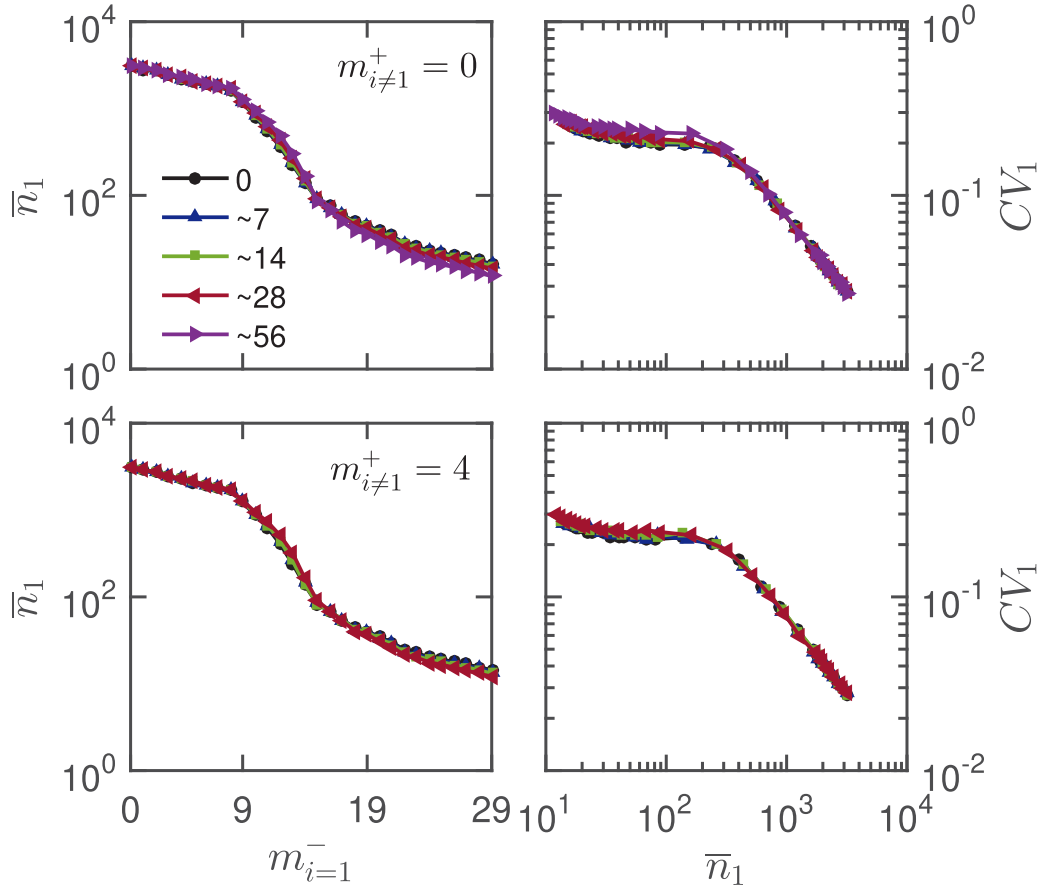


FIG. 13. Ultrasensitivity (left) and biphasic scaling (right) of node 1 in networks with removed interactions. The percentage reduction of mutual interactions on all other nodes is indicated inside the plot. Top row: $m_{i \neq 1}^+ = 0$ and bottom row: $m_{i \neq 1}^+ = 4$. In all cases the values of \bar{a}_+ and \bar{a}_- were 0.001 and 0.001, respectively.

strength ($\max m_{i=1}^-$) with \bar{a}_- further bolstered the conclusion that negative interaction reduces the strength of the intrinsic noise. Moreover, the anticorrelation between $\max m_{i=1}^-$ and \bar{a}_- reveals that the noise can be minimized either by a large number of weak negative interactions or by small number of strong negative regulations.

Our entire set of calculations were based on the fully connected democratic network, where every node interacts with the every other node in the network. However, in practice the networks are often sparse in nature generating functional behavior relevant to cellular physiology (reviewed in Ref. [50]). Therefore in order to investigate the properties of similar networks with lesser connectivities, we reduced the number of mutual interactions by randomly knocking out a certain number of interactions keeping the interaction between node 1 and all other nodes intact ($a_{1,j} \neq 0$ and $a_{i,1} \neq 0$). These reduced networks exhibited similar qualitative behavior of the average and the intrinsic noise as was the case of fully connected networks (Fig. 13). Therefore partially connected networks also behave in the same way as the fully connected democratic networks.

B. Extrinsic noise

In addition to intrinsic noise, chemical reactions inside living cells are also subjected to various sources of extrinsic

noise. We next investigated the extrinsic noise in democratic networks with a varying number of negative and positive interactions [4,6–9,51]. In order to simulate extrinsic noise, we created an ensemble of 5000 networks where each network has a different strength of mutual interactions ($a_{i,j}$) for a given pair of nodes. For a given average strength of negative or positive interaction, we sampled the individual interaction strength values ($a_{i,j}$) from log-normal distribution with CV of 0.3 [12,42,52]. Then we solved the deterministic differential equations (1) of 5000 replica of networks and estimated the steady-state statistical properties of the variables in the network. Therefore the values of $a_{i,j}$ were different in every run.

To determine the regulation of extrinsic noise by the qualitative nature of interactions, we performed analyses analogous to those we have done in the case of intrinsic noise. In Fig. 14 we plotted the variation of average [Fig. 14(a)] and CV [Fig. 14(b)] of node 1 with the number of negative interactions on node 1 and the number of positive interactions on all other nodes in the network. Similar to the intrinsic noise case, the average abundance of node 1 sharply decreased to a very small value beyond a certain number of negative interactions on node 1. Similar qualitative dependence of \bar{n}_1 with $m_{i=1}^-$ occurred with increasing values of $m_{i \neq 1}^+$. Analogous to the intrinsic noise case, the average was also dependent on the values of \bar{a}_- and \bar{a}_+ (not shown). The surface plot of CV₁ with

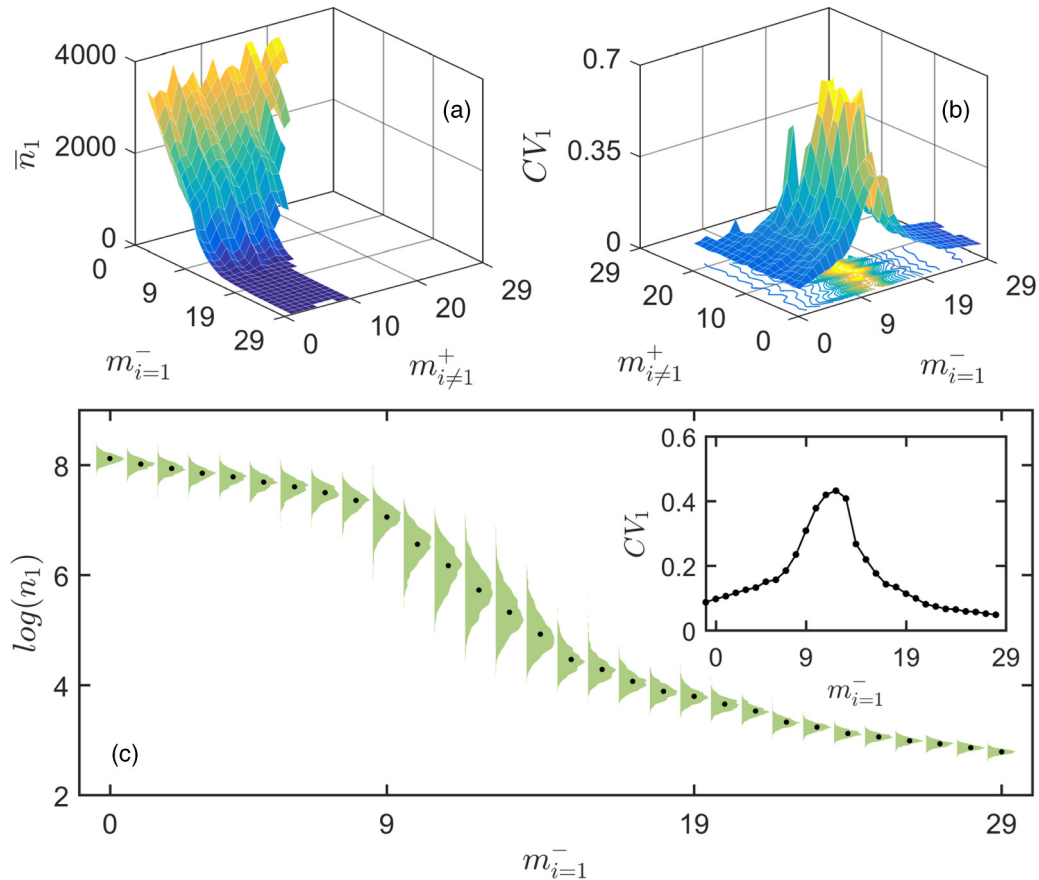


FIG. 14. Surface plot of \bar{n}_1 (a) and CV_1 (b) as function of $m_{i=1}^-$ and $m_{i\neq 1}^+$ in the network having $d_N = 30$ with extrinsic noise. (c) Variation of distribution of abundance of node 1 with $m_{i=1}^-$ for the network with $m_{i\neq 1}^+ = 0$. In the inset the dependence of CV on $m_{i=1}^-$ is shown for the same network. The other parameters were $\bar{a}_- = 0.001$ and $\bar{a}_+ = 0.001$. The dots indicate the average abundance.

$m_{i=1}^-$ and $m_{i\neq 1}^+$ indicated that the behavior of noise was starkly different from that of the case in the intrinsic noise. Here with $m_{i=1}^-$, the noise passed through a maximum indicating that the variability was maximum with intermediate number of incoming negative interactions on node 1. From Fig. 14(a) and Fig. 14(b), it appeared that the maximum in noise and the sharp change in average happened around the same value of $m_{i=1}^-$. In order to determine the reason for the maximum in the noise, in Fig. 14(c) we plotted the variation of distributions of node 1 as function of $m_{i=1}^-$ for the network with $m_{i\neq 1}^+ = 0$. We found that the width of the distributions was quite narrow in the extreme ends of the $m_{i=1}^-$, whereas the width of these distributions was quite high in the intermediate $m_{i=1}^-$. It is also apparent from the plot that the average exhibited somewhat ultrasensitive dependence with $m_{i=1}^-$. Owing to this ultrasensitive nature, around the critical point where abundance drops from high to low value, the system became more sensitive to extrinsic noise resulting in increased noise in the intermediate values of $m_{i=1}^-$.

As pointed out before, the dependence of CV on the average is an important aspect of chemical noise in biochemical reaction networks. Therefore in order to determine the dependence of extrinsic noise on the average, in Fig. 15(a) we plotted CV of node 1 as a function of its average. The opposite of the intrinsic noise, here noise passed through maxima with the average. This dependence CV_1 with \bar{n}_1 is consistent with

the variation of CV_1 with $m_{i\neq 1}^+$ [Fig. 14(b)]. As opposed to the intrinsic noise where CV always decreased with the

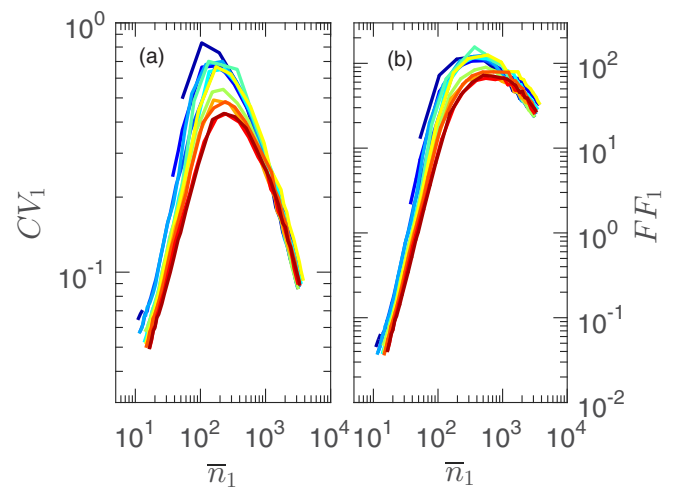


FIG. 15. Variation of noise (a) and noise strength (b) of node 1 as function of average (\bar{n}_1). Different lines represent different values of $m_{i\neq 1}^+$: from red ($m_{i\neq 1}^+ = 0$) to blue ($m_{i\neq 1}^+ = 11$) the value of $m_{i\neq 1}^+$ increases by 1. The other parameters were $\bar{a}_- = 0.001$ and $\bar{a}_+ = 0.001$.

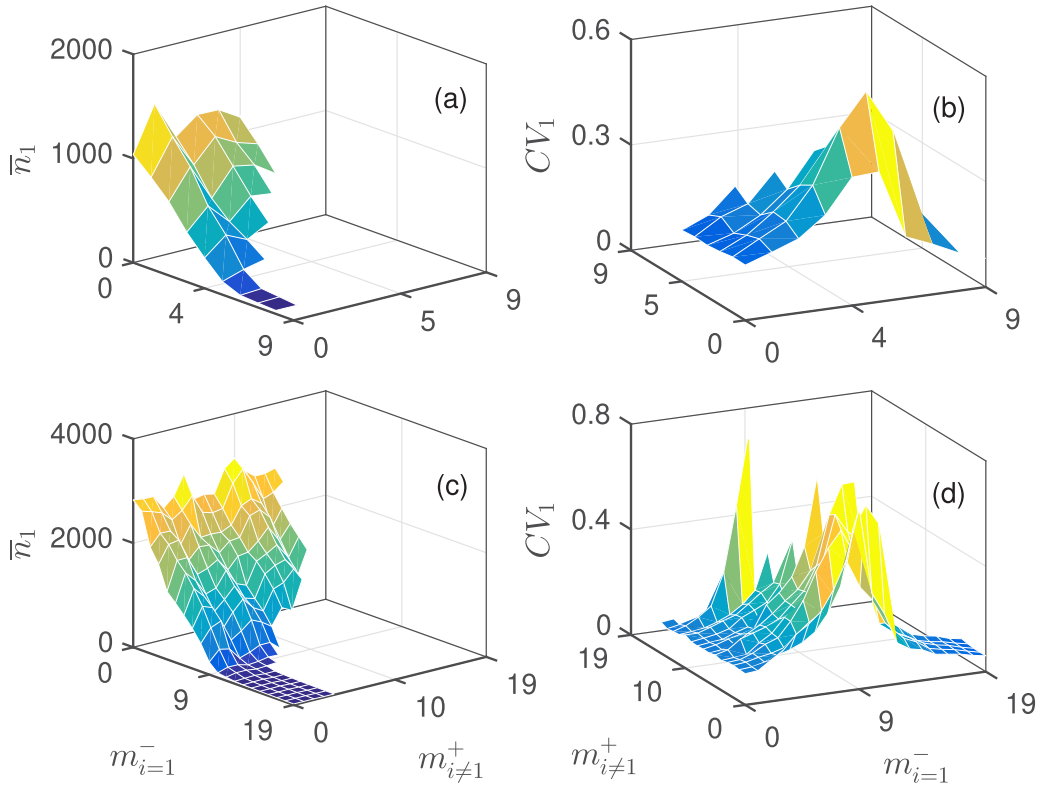


FIG. 16. Surface plot of the average abundance and CV of node 1 for the networks with 10 (top row) and 20 (bottom row) nodes as a function of number of $m_{i=1}^-$ and $m_{i\neq 1}^+$ under extrinsic noise. The other parameters were the same as in Fig. 14.

average, here in the case of extrinsic noise, it increases with the average in the low to intermediate regime of average abundance. The consequence of this type of variation is that, with only extrinsic noise, the network can have low noise even with very low molecular abundance. This is in contrast to the intrinsic noise where the system will be noisy in the limit of low population abundance. As we did in the case of intrinsic noise, here also we verified that the results were consistent for networks with different sizes. In Fig. 16 we report the variation of average and noise on the $m_{i=1}^-$ and $m_{i\neq 1}^+$ for networks with 10 and 20 nodes.

As in the case of intrinsic noise, we determined the dependence of the average strength of negative and positive interactions on variability. In this context, in Fig. 17(a) we plotted the dependence of maximum CV (the peak of the line in Fig. 15) of node 1 with the average strength of the negative interactions (\bar{a}_-) for networks with $m_{i\neq 1}^+ = 0$. The maximum noise decreases with the average strength of negative interaction indicating that negative regulation was responsible for attenuating the effect of extrinsic variability. Further the anticorrelation between the number of negative interaction on node 1 corresponding to the maximum noise ($^{max}m_{i=1}^-$) and average strength of negative interaction points out the compensatory effect of negative interaction in attenuating noise [Fig. 17(b)]. These plots also exhibited that the increased positive interactions lead to amplification of extrinsic noise in the democratic network. In the entire calculations we have chosen log-normal distribution of strengths of interaction ($a_{i,j}$). However, we have verified that the general properties

of the networks do not depend on the specific choice of the log-normal distribution of $a_{i,j}$. In Fig. 18 we show that the qualitative dependence of average and noise remained similar with the Gaussian distribution of $a_{i,j}$ for both the intrinsic and extrinsic noise.

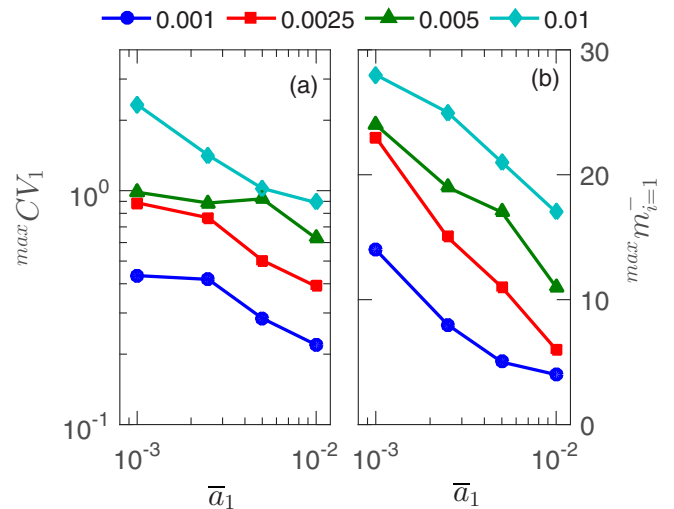


FIG. 17. (a) Dependence of maximum noise ($^{max}CV_1$) with \bar{a}_- for $m_{i\neq 1}^+ = 0$. (b) Variation of $^{max}m_{i=1}^-$, the number of negative interaction on node 1 corresponding to the maximum noise, with \bar{a}_- . Different lines represent different values of \bar{a}_+ .

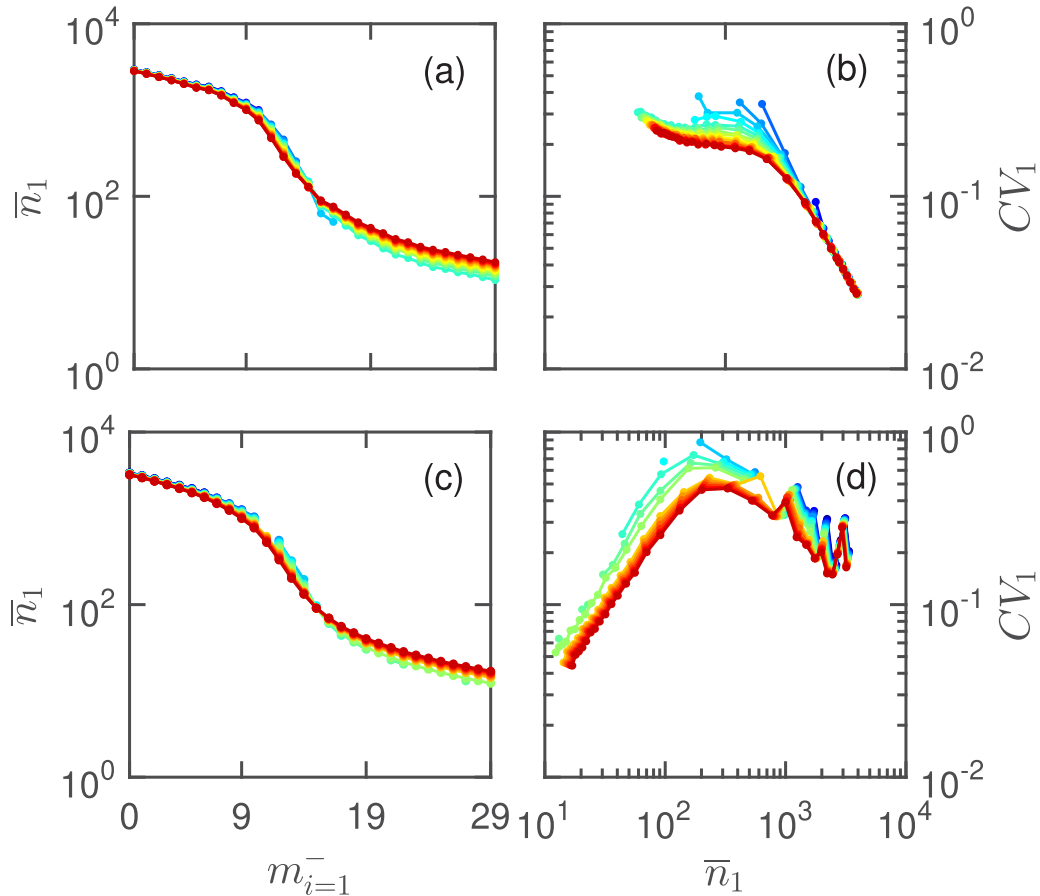


FIG. 18. Plot of \bar{n}_1 vs $m_{i=1}^-$ (a and c) and CV_1 vs \bar{n}_1 (b and d). Top row: intrinsic noise; bottom row: extrinsic noise. The values of $a_{i,j}$ were chosen from Gaussian distributions with $\bar{a}_- = 0.001$ and $\bar{a}_+ = 0.001$ and $CV = 0.3$ in both cases. Different lines represent different values of $m_{i \neq 1}^+$: from red ($m_{i \neq 1}^+ = 0$) to blue ($m_{i \neq 1}^+ = 15$) the value of $m_{i \neq 1}^+$ increases by 1.

III. CONCLUSION

The fluctuations of molecular abundance of a finite number of macromolecular species and variation of different extrinsic factors both contribute to observed cellular heterogeneity in single-cell and multicellular organisms [1,2]. Statistical mechanical models of gene expression noise have proven to be successful in providing quantitative explanation of observed variability in protein abundance [53]. Further models have explored the roles of feedback regulations in noise propagation either in standalone genes or in networks of genes [20,22,53]. System-level models of cellular physiology, such as the cell cycle, have determined the crucial aspects of positive feedback loops and average lifetime of molecular species in attenuating chemical noise [32,54]. However, how chemical noise is regulated in a generalized chemical reaction network has not been investigated thus far, to the best of our knowledge. Particularly in the context of organisms' response to external cues, one must acknowledge that a well-coordinated effort of a host of interconnected genes leads to a suitable response [45,46]. In view of this, we investigated the propagation of intrinsic and extrinsic noise in a democratic chemical network where every node in the network is connected to the rest of the nodes by either positive or negative interactions. Our main objective here was to determine the role of the qualitative and

quantitative nature of interactions in dictating the variability of the chemical species in the network.

Using the mass action rate law of chemical reactions, we modeled a democratic chemical network consisting of 30 interconnecting nodes. We studied intrinsic noise using Gillespie's SSA. We found that the noise, estimated by the coefficient of variation, rapidly switched from low to high with the increase of number in negative interactions on the node of interest. Importantly, this qualitative behavior of noise was mostly independent of the qualitative nature of interactions acting on the other nodes in the network. We attributed the switching of noise to the weak ultrasensitive switching of the average. Ultrasensitivity is a typical property of nonlinear reaction networks. However, our calculations exhibited that a democratic network with linear kinetics can also behave in an ultrasensitive manner. Our analyses demonstrated a biphasic power-law scaling (with two distinct scaling exponents) of noise with average. The values of these two exponents were critically dependent on the strength of the interactions. Unlike the noise, noise strength, however, passed through a maxima with the average. Simulation results showed that the noise strength decreased with the strength of the negative interactions, whereas the strength of positive interaction had the opposite effect. Therefore it is fair to conclude that negative

interactions attenuate the effect of intrinsic noise and positive interactions amplify the noise.

In order to investigate the extrinsic noise, we executed deterministic simulations of an ensemble of networks where the strengths of mutual interactions of interconnected nodes were chosen from log-normal distributions. In the extrinsic noise, the dependence of noise with the average was found to be different compared to the intrinsic noise case. Here with the average the noise passed through a maximum indicating that variability was highest in the intermediate number of negative interactions. The consequence of this type of variation is that, with only extrinsic noise, the network can have low noise even with very low molecular abundance. This is in contrast to the intrinsic noise where the system will be noisy in the limit of low population abundance. Therefore the effect of negative interactions regulating noise can be quite different depending on the sources of noise (intrinsic or extrinsic). Finally the reduction of maximum noise with the average strength of negative interactions indicates that negative regulations dampen the extrinsic noise.

We have used mass action rate laws of chemical reactions to model the democratic networks. However, often nonlinear rate laws such as Hill function and Michaelis-Menten kinetics

are routinely used in both protein interaction and gene regulatory networks to benchmark the mathematical models with the experimental observations. Our use of mass action rate laws allowed us to estimate intrinsic chemical noise accurately using Gillespie's SSA. Further it ruled out the possibility of nonlinear phenomena such as multistability and oscillations in the networks. Mass-action-based modeling of protein interaction networks has gained popularity as it accurately predicts the effects of intrinsic chemical noise in the reaction networks [32,54–59]. In the future it will be worthwhile to investigate the propagation of noise in networks with nonlinear rate laws using approximate simulation methods such as the chemical Langevin equation.

ACKNOWLEDGMENTS

The work was supported by funding from the Science and Engineering Research Board, Department of Science and Technology (India), Grant No. EMR/2015/001899, to D.B. S.D. acknowledges support from a fellowship from the INSPIRE program of the Department of Science and Technology, India.

-
- [1] A. Raj and A. van Oudenaarden, *Cell* **135**, 216 (2008).
 - [2] A. Sanchez, S. Choubey, and J. Kondev, *Annu. Rev. Biophys.* **42**, 469 (2013).
 - [3] E. M. Ozbudak, M. Thattai, I. Kurtser, A. D. Grossman, and A. van Oudenaarden, *Nat. Genet.* **31**, 69 (2002).
 - [4] M. B. Elowitz, A. J. Levine, E. D. Siggia, and P. S. Swain, *Science* **297**, 1183 (2002).
 - [5] W. J. Blake, M. Kærn, C. R. Cantor, and J. J. Collins, *Nature (London)* **422**, 633 (2003).
 - [6] J. M. Raser and E. K. O'Shea, *Science* **304**, 1811 (2004).
 - [7] D. Volfson, J. Marciniak, W. J. Blake, N. Ostroff, L. S. Tsimring, and J. Hasty, *Nature (London)* **439**, 861 (2006).
 - [8] D. Huh and J. Paulsson, *Nat. Genet.* **43**, 95 (2011).
 - [9] M. S. Sherman, K. Lorenz, M. H. Lanier, and B. A. Cohen, *Cell Syst.* **1**, 315 (2015).
 - [10] D. Das, S. Dey, R. C. Brewster, and S. Choubey, *PLoS Comput. Biol.* **13**, e1005491 (2017).
 - [11] S. D. Talia, J. M. Skotheim, J. M. Bean, E. D. Siggia, and F. R. Cross, *Nature (London)* **448**, 947 (2007).
 - [12] S. L. Spencer, S. Gaudet, J. G. Albeck, J. M. Burke, and P. K. Sorger, *Nature (London)* **459**, 428 (2009).
 - [13] O. Feinerman, J. Veiga, J. R. Dorfman, R. N. Germain, and G. Altan-Bonnet, *Science* **321**, 1081 (2008).
 - [14] N. Geva-Zatorsky, N. Rosenfeld, S. Itzkovitz, R. Milo, A. Sigal, E. Dekel, T. Yarnitzky, Y. Liron, P. Polak, G. Lahav, and U. Alon, *Mol. Syst. Biol.* **2**, 2006.0033 (2006).
 - [15] A. Eldar and M. B. Elowitz, *Nature (London)* **467**, 167 (2010).
 - [16] G. Balázsi, A. van Oudenaarden, and J. J. Collins, *Cell* **144**, 910 (2011).
 - [17] L. S. Weinberger, J. C. Burnett, J. E. Toettcher, A. P. Arkin, and D. V. Schaffer, *Cell* **122**, 169 (2005).
 - [18] M. Acar, J. T. Mettetal, and A. van Oudenaarden, *Nat. Genet.* **40**, 471 (2008).
 - [19] T. Çağatay, M. Turcotte, M. B. Elowitz, J. Garcia-Ojalvo, and G. M. Süel, *Cell* **139**, 512 (2009).
 - [20] M. Thattai and A. van Oudenaarden, *Proc. Natl. Acad. Sci. USA* **98**, 8614 (2001).
 - [21] J. Paulsson, *Nature (London)* **427**, 415 (2004).
 - [22] J. Pedraza and A. van Oudenaarden, *Science* **307**, 1965 (2005).
 - [23] N. Friedman, L. Cai, and X. S. Xie, *Phys. Rev. Lett.* **97**, 168302 (2006).
 - [24] V. Shahrezaei and P. S. Swain, *Proc. Natl. Acad. Sci. USA* **105**, 17256 (2008).
 - [25] J. M. Pedraza and J. Paulsson, *Science* **319**, 339 (2008).
 - [26] T. Jia and R. V. Kulkarni, *Phys. Rev. Lett.* **106**, 058102 (2011).
 - [27] M. Shreshtha, A. Surendran, and A. Ghosh, *Phys. Biol.* **13**, 036004 (2016).
 - [28] A. Becskei and L. Serrano, *Nature (London)* **405**, 590 (2000).
 - [29] F. J. Bruggeman, N. Blüthgen, and H. V. Westerhoff, *PLoS Comput. Biol.* **5**, e1000506 (2009).
 - [30] M. Hinczewski and D. Thirumalai, *J. Phys. Chem. B* **120**, 6166 (2016).
 - [31] G. Hornung and N. Barkai, *PLoS Comput. Biol.* **4**, e8 (2008).
 - [32] D. Barik, D. A. Ball, J. Peccoud, and J. J. Tyson, *PLoS Comput. Biol.* **12**, e1005230 (2016).
 - [33] M. Thattai and A. van Oudenaarden, *Biophys. J.* **82**, 2943 (2002).
 - [34] P. S. Swain, *J. Mol. Biol.* **344**, 965 (2004).
 - [35] S. Hooshangi, S. Thiberge, and R. Weiss, *Proc. Natl. Acad. Sci. USA* **102**, 3581 (2005).
 - [36] O. Brandman, J. E. Ferrell, R. Li, and T. Meyer, *Science* **310**, 496 (2005).
 - [37] R. Maithreye and S. Sinha, *Phys. Biol.* **4**, 48 (2007).
 - [38] H. Zhang, Y. Chen, and Y. Chen, *PLoS ONE* **7**, e51840 (2012).
 - [39] M. S. Avendaño, C. Leidy, and J. M. Pedraza, *Nat. Commun.* **4**, 2605 (2013).

- [40] S. R. Chepyala, Y.-C. Chen, C.-C. S. Yan, C.-Y. D. Lu, Y.-C. Wu, and C.-P. Hsu, *Sci. Rep.* **6**, 23607 (2016).
- [41] C. Briat, A. Gupta, and M. Khammash, *Cell Syst.* **2**, 15 (2016).
- [42] A. Dey and D. Barik, *PLoS ONE* **12**, e0188623 (2017).
- [43] G. Chalancon, C. N. Ravarani, S. Balaji, A. Martinez-Arias, L. Aravind, R. Jothi, and M. M. Babu, *Trends Genet.* **28**, 221 (2012).
- [44] N. Bhardwaj, K.-K. Yan, and M. B. Gerstein, *Proc. Natl. Acad. Sci. USA* **107**, 6841 (2010).
- [45] R. Jothi, S. Balaji, A. Wuster, J. A. Grochow, J. Gsponer, T. M. Przytycka, L. Aravind, and M. M. Babu, *Mol. Syst. Biol.* **5**, 294 (2009).
- [46] Y. Bar-Yam, D. Harmon, and B. de Bivort, *Science* **323**, 1016 (2009).
- [47] D. T. Gillespie, *J. Comput. Phys.* **22**, 403 (1976).
- [48] J. E. Ferrell and S. H. Ha, *Trends Biochem. Sci.* **39**, 496 (2014).
- [49] J. J. Tyson, K. C. Chen, and B. Novak, *Curr. Opin. Cell Biol.* **15**, 221 (2003).
- [50] O. Martin, A. Krzywicki, and M. Zagorski, *Phys. Life Rev.* **17**, 124 (2016).
- [51] V. Shahrezaei, J. F. Ollivier, and P. S. Swain, *Mol. Syst. Biol.* **4**, 196 (2008).
- [52] R. Ahrends, A. Ota, K. M. Kovary, T. Kudo, B. O. Park, and M. N. Teruel, *Science* **344**, 1384 (2014).
- [53] J. Paulsson, *Phys. Life Rev.* **2**, 157 (2005).
- [54] D. Barik, W. T. Baumann, M. R. Paul, B. Novak, and J. J. Tyson, *Mol. Syst. Biol.* **6**, 405 (2010).
- [55] S. Kar, W. T. Baumann, M. R. Paul, and J. J. Tyson, *Proc. Natl. Acad. Sci. USA* **106**, 6471 (2009).
- [56] O. Kapuy, D. Barik, M. R. Domingo Sananes, J. J. Tyson, and B. Novak, *Prog. Biophys. Mol. Biol.* **100**, 47 (2009).
- [57] W. W. Chen, B. Schoeberl, P. J. Jasper, M. Niepel, U. B. Nielsen, D. A. Lauffenburger, and P. K. Sorger, *Mol. Syst. Biol.* **5**, 239 (2009).
- [58] K. Iwamoto, Y. Shindo, and K. Takahashi, *PLoS Comput. Biol.* **12**, e1005222 (2016).
- [59] K. M. Kovary, B. Taylor, M. L. Zhao, and M. N. Teruel, *Mol. Syst. Biol.* **14**, e7997 (2018).